

1 **Distribution and stable carbon isotopic composition of dicarboxylic**
2 **acids, ketocarboxylic acids and α -dicarbonyls in fresh and aged**
3 **biomass burning aerosols**

4
5 Minxia Shen^{1,2}, Kin Fai Ho^{3,4}, Wenting Dai¹, Suixin Liu¹, Ting Zhang¹, Qiyuan Wang¹,
6 Jingjing Meng⁵, Judith C. Chow^{1,6}, John G. Watson^{1,6}, Junji Cao^{1*}, Jianjun Li^{1,7*}

7
8 ¹State Key Laboratory of Loess and Quaternary Geology, Key Lab of Aerosol
9 Chemistry and Physics, Institute of Earth Environment, Chinese Academy of
10 Sciences, Xi'an 710061, China;

11 ²University of Chinese Academy of Sciences, Beijing, China;

12 ³The Jockey Club School of Public Health and Primary Care, The Chinese University
13 of Hong Kong, Hong Kong, China;

14 ⁴Shenzhen Municipal Key Laboratory for Health Risk Analysis, Shenzhen Research
15 Institute, The Chinese University of Hong Kong, Shenzhen, China;

16 ⁵School of Geography and the Environment, Liaocheng University, Liaocheng
17 252000, China;

18 ⁶Division of Atmospheric Sciences, Desert of Research Institute, Reno, Nevada, USA;

19 ⁷CAS Center for Excellence in Quaternary Science and Global Change, Xi'an 710061,
20 China.

21
22
23
24 *Corresponding author: Jianjun Li, e-mail address: lijj@ieecas.cn;

25 Junji Cao, e-mail address: cao@loess.llqg.ac.cn

26

27 **Abstract**

28 Biomass burning (BB) is a significant source for dicarboxylic acids (diacids) and
29 related compounds that play important roles in atmospheric chemistry and climate
30 change. In this study, a combustion chamber and oxidation flow reactor were used to
31 generate fresh and aged aerosols from burned rice, maize, and wheat straw to
32 investigate atmospheric aging and the stable carbon isotopic ($\delta^{13}\text{C}$) composition of
33 these emissions. Succinic acid (C_4) was the most abundant species in fresh samples;
34 while, oxalic acid (C_2) became dominant after atmospheric aging. Of all diacids, C_2
35 had the highest aged to fresh emission ratios (A/F), suggesting that C_2 is largely
36 produced through secondary photochemical processes. Compared with fresh samples,
37 the emission factors of ketocarboxylic acids and α -dicarbonyls increased after 2-day
38 but decreased after 7-day aging, indicating short residence time and further
39 atmospheric degradation from 2- to 7-days. The $\delta^{13}\text{C}$ values of C_2 for aged biomass
40 samples were higher than those of urban aerosols but lower than marine or mountain
41 aerosols, and the $\delta^{13}\text{C}$ values of C_2 became isotopically heavier during aging.
42 Relationships between the reduction in volatile organic compounds (VOCs), such as
43 toluene, benzene, and isoprene, and increase in diacids after 2-day aging indicate that
44 these VOCs led to the formation of diacids. However, no significant correlation was
45 found between decreases in VOCs and increases in 7-day aged diacids. In
46 addition, the A/F of C_2 was 50.8 at 2 days and 64.5 at 7 days, indicating that the
47 conversion of VOCs to C_2 was almost completed within 2 days. For the longer aging
48 times, the particulate phase compounds may undergo further degradation in the
49 oxidation processes.

50 **Keywords:** Biomass burning, Dicarboxylic acids, Atmospheric aging, Stable carbon
51 isotope, VOCs

52 **1. Introduction**

53 Dicarboxylic acids (diacids), ketocarboxylic acids and α -dicarbonyls are
54 common components of the atmospheric organic aerosol, accounting for 1–3% of the
55 total organic carbon in urban areas and >10% of the carbon mass in remote regions
56 (Kawamura and Usukura, 1993; Kawamura and Sakaguchi, 1999; Kerminen et al.,
57 2000; Zhao et al., 2018). Due to their high water-solubility and other physicochemical
58 properties, diacids affect the hygroscopic growth of particulate matter (PM), and these
59 compounds are involved in the activation of cloud condensation nuclei and formation
60 of ice nuclei (Kawamura and Bikkina, 2016). Diacids and related compounds have
61 been found in a wide variety of environments including urban settings (Ho et al., 2006;
62 Kawamura and Ikushima, 1993; Meng et al., 2020; Sorathia et al., 2018; Wang et al.,
63 2002, 2006, 2012), mountains ranges (Kawamura et al., 2013; Kunwar et al., 2019),
64 and remote marine atmospheres (Hoque et al., 2020; Kawamura and Usukura, 1993).
65 They also have been reported in both the Arctic and Antarctic aerosols (Kawamura et
66 al., 1996 a, b; Narukawa et al., 2002, 2003) as well as polar ice cores (Legrand and De
67 Angelis, 1996; Kawamura et al., 2001). Various studies have assessed the molecular
68 distributions, temporal variability, and sources of diacids in different air-sheds.

69 There are both primary and secondary sources for diacids (Mkoma and
70 Kawamura, 2013). Primary sources include emissions from fossil fuel combustion
71 (Kawamura and Kaplan, 1987; Rogge et al., 1993), cigarette burning (Rogge et al.,
72 1994), cooking (Rogge et al., 1991), and biomass burning (BB) (Narukawa et al.,
73 1999; Schauer et al., 2001). Of these, BB was found to be an important source of
74 diacids and related compounds over regional and global scales (Kundu et al., 2010).
75 Emissions from BB not only compose a major source of primary particles but also
76 introduce aerosol precursors to the atmosphere (Akagi et al., 2011; Gilman et al., 2015;
77 Reid et al., 2005). Secondary sources include particles produced by
78 chemical/photochemical oxidation reactions of volatile organic compounds (VOCs),
79 especially those emitted from primary sources (Lim et al., 2013; Carlton et al., 2006,
80 2007).

81 Being one of the major contributors to the global budget of aerosols, BB
82 emissions are of particular concern because they impact air quality, visibility, climate,
83 and human health (Hodshire et al., 2019). As the largest developing country and one
84 that burns large quantities of biomass, China has long suffered from severe air
85 pollution from BB (Chen et al., 2016; Fullerton et al., 2008). Domestic crop residues
86 (eg. rice, maize, and wheat straw) and firewood are the most significant energy
87 sources in most rural areas, and these are commonly used for cooking and heating (Li
88 et al., 2021; Tao et al., 2018).

89 Diacids, ketocarboxylic acids and α -dicarbonyls are products of BB (Agarwal et
90 al., 2010). Although these acids have been measured in ambient air in some areas
91 dominated by BB sources (FaLkovich et al., 2005; Kundu et al., 2010; Kawamura et
92 al., 2013), there have been few BB sources emission (e.g., chamber) measurements. It
93 was reported that BB smokes was found to contain large amounts of gaseous
94 pollutants, such as VOCs, nitrogen oxides (NO_x), sulfur dioxide (SO₂), and ammonia
95 (NH₃) (Akagi et al., 2011; Andreae and Merlet, 2001). Gas-phase compounds,
96 especially VOCs, can be partition to the particle phase through nucleation,
97 condensation, and heterogeneous chemical reactions, creating secondary organic
98 aerosol (SOA) and adding to aerosol mass (Hodshire et al., 2019; Lim et al., 2019).
99 Oxalic acid (C₂), the most abundant species of diacids (Kawamura and Sakaguchi,
100 1999) and is formed by various VOCs in cloud droplets through photochemical
101 oxidation and liquid phase reactions. It is of interest to quantify emission factors (EFs)
102 of diacids and related compounds during the combustion of different biomass fuels in
103 the laboratory. Kalogridis et al. (2018) performed small-scale fire experiments using
104 the Large Aerosol Chamber (LAC, 1800 m³) with a focus on BB from Siberian boreal
105 coniferous forests, and presented experimental data on EFs of diacids. However, this
106 study only focused on the EFs of diacids of fresh pollutants that directly emitted from
107 BB, so it is necessary to further investigation of molecular composition of aged BB
108 aerosols. In addition, limited data are available on the specific diacids emitted from
109 burning of agricultural residues. Therefore, it is important to investigate the molecular
110 composition of diacids in both fresh and aged BB aerosols to advance current

111 understanding of the potential environmental and climatic effects.

112 In this study, rice, maize, and wheat straw were selected for laboratory
113 simulations of fresh and aged BB aerosols. The study was conducted with the use of a
114 combustion chamber and oxidation flow reactor (OFR). Fresh and aged BB aerosols
115 were chemically analyzed for molecular characteristics and the stable carbon isotopic
116 composition ($\delta^{13}\text{C}$) of selected diacids, ketocarboxylic acids, α -dicarbonyls, and
117 benzoic. The objectives of this study were to (1) investigate the emissions of diacids,
118 ketocarboxylic acids and α -dicarbonyls from crop residue burning; (2) evaluate the
119 effects of atmospheric aging processes on diacids and related compounds; and (3)
120 investigate relationship between VOCs with C_2 and intermediates that form in the
121 aging process to explore potential formation mechanisms of selected organic acids.

122 **2. Methods**

123 **2.1. Preparation and collection of fresh and aged BB aerosols**

124 The experimental setup is illustrated in supplementary Fig. S1. Detailed
125 procedures for sample preparation and collection may be found in previous studies (Li
126 et al., 2020, 2021; Niu et al., 2020). Briefly, fresh smoke was generated by burning
127 dry biomass fuels (i.e., rice, maize, and wheat straw) in a combustion chamber, and
128 the smoke was then passed through a Potential Aerosol Mass-Oxidation Flow
129 Reaction (PAM-OFR) (Aerodyne Research, LLC, Billerica, MA, USA) to simulate
130 aging processes in timescale of hours to days. The biomass combustion chamber with
131 a volume of $\sim 8 \text{ m}^3$ (1.8m (W) \times 1.8m (L) \times 2.2m (H)), which was made of 3 mm thick
132 aluminum to withstand high-temperature heating. The combustion chamber was
133 equipped with a thermoanemometer, an air purification system, a heated sampling line,
134 a dilution sampler, and so on. More detailed information about the design and
135 evaluation of combustion chamber were described in Tian et al. (2015).

136 In order to get sufficient aerosols samples for measurements of chemical
137 composition, around 1 kg biomass fuels were burned inside the chamber in 10 burning
138 cycles. The entire burning cycle, including ignition, flaming, smoldering, and
139 extinction, intends to simulate real-world source characterization. Each burning cycle,

140 containing ~100 g biomass fuels, lasts around 12~18 min. The fresh smoke was
141 diluted by 4.6 times using clean air controlled by the flow balance. A portion of the
142 diluted smoke by dilution sampler (Model 18, Baldwin Environmental Inc., Reno, NV,
143 USA) was drawn through a quartz fiber filter (47 mm diameter, Whatman QM/A,
144 Maidstone, UK) at 5 L min⁻¹ using a mini-Vol PM_{2.5} sampler (Airmetrics, OR, USA)
145 to capture fresh emission.

146 The PAM-OFR can be used to simulate an environment with extremely high
147 oxidant concentrations with short residence times (Kang et al., 2007). Another portion
148 of the exhaust (~9 L min⁻¹) was directed through a 19-L cylinder PAM-OFR (with a
149 diameter of 20 cm and length of 60 cm) to simulate atmospheric aging. Residence
150 time of PAM-OFR is estimated to be 90 ± 1 s at flow rate of 9 L min⁻¹ (Li et al., 2021).
151 Three oxidants (O₃, •OH, and •HO₂) were generated in the PAM chamber using
152 irradiation from ultraviolet (UV) lamps. The OH exposure values (OH_{exp}) can be
153 calculated by the concentration of SO₂ and CO at the OFR inlet and outlet in a
154 laboratory setting. Relative humidity (RH) inside the OFR was varied by passing
155 different amounts of carrier gas through the OFR humidifier (MH-110). Additional
156 details on smoke generation condition, test study and evaluation of the PAM-OFR
157 were described by Cao et al. (2020).

158 In this study, the UV lamps operated at a voltage of 2 and 3.5 V, OH_{exp} in the
159 chamber were estimated at 2.6 × 10¹¹ and 8.8 × 10¹¹ molecules-sec/m³, respectively.
160 These levels corresponded to ~2 and 7 day of aging (Chow et al., 2019; Watson et al.,
161 2019), assuming a representative atmospheric •OH level of 1.5 × 10⁶ molecules/m³
162 (Mao et al., 2009). The aged aerosols were sampled by another mini-Vol PM_{2.5}
163 sampler (5 L min⁻¹) following the reactions in the PAM-OFR chamber. Each test was
164 conducted in triplicate to account for experimental errors and to provide a measure of
165 variability, which was calculated as standard deviations. A total of 36 samples were
166 collected and analyzed for chemical composition.

167 **2.2. Sample extraction, derivatization, and quantification**

168 For diacids, ketocarboxylic acids and α-dicarbonyls analyzing, one quarter of
169 each filter sample was extracted three times (15 min each) with purified (18.2 MΩ)

170 water (Milli-Q, Merch, France) and ultrasonication. The pH of the aerosol extracts
171 was adjusted to 8.5 to 9.0 using a 0.1 M potassium hydroxide solution prior to drying
172 that convert carboxylic acids into their salts (Bikkina et al., 2021). This drying step
173 improves the recovery of smaller diacids, such as C₂ (Hegde and Kawamura, 2012).
174 Water extracts were concentrated to near dryness with a rotary evaporator under
175 vacuum and then reacted with 14% BF₃/n-butanol at 100 °C for 1 h to derivatize
176 carboxyl groups to dibutyl esters and oxo groups to dibutoxyacetals.

177 After derivatization, n-hexane was added and washed with pure water three times
178 to remove the water-soluble inorganics such as hydrogen fluoride and boric acid. The
179 hexane layer was concentrated to near dryness using a rotary evaporator under
180 vacuum and a N₂ blow-down technique, and then the esters and acetals of target
181 analytes were dissolved in known amounts of n-hexane. Finally, the hexane layers
182 were concentrated to 100 µL and analyzed using a capillary gas chromatography (GC;
183 HP 6890, Agilent Technology, Santa Clara, CA, USA) equipped with a split/splitless
184 injector and a flame ionization detector (FID). Peak identification was performed by
185 comparing the GC retention times with those of authentic standards and confirmed by
186 a thermal desorption (TD) unit coupled with a gas chromatograph/mass spectrometric
187 detector (TD-GC/MS, Models 7890A/5975C, Agilent Technology, Santa Clara, CA,
188 USA). The detection limits for those organic compounds were 0.1 ng m⁻³, and the
189 analytical errors, based on the replicate analyses, were less than 15%. Recoveries of
190 the target compounds were 83% for C₂ and 87% to 110% for the other species.

191 **2.3. Emission factor calculations**

192 Concentrations of the various species in the aged samples were affected by their
193 initial emission, also undergo degradation and production through secondary chemical
194 processes. Fresh and aged fuel-based EF_s for each measured chemical compound
195 were calculated by dividing its filter mass by the mass of combusted dry biomass fuel
196 (Andreae and Merlet, 2001; Li et al., 2020; Tian et al., 2015); that is:

$$197 \quad EF_i = \frac{m_i \times v_{Stk} \times D \times t_{sample}}{Q_p \times m_{fuel}} \times DR$$

198 where EF_i (mg kg⁻¹) is the EF of chemical compound i for the specific crop; m_i (mg)

199 is the mass of chemical compound *i* collected on the filter; v_{stk} is the average stack
200 flow velocity ($m\ s^{-1}$) at standard conditions; D is the stack cross section (m^2); t_{sample} is
201 the sampling duration (s); Q_p is the sampling volume through the filter (m^3) at
202 standard temperature and pressure; and m_{fuel} is the mass of burned biomass fuel (kg,
203 dry weight).

204 The dilution ratio (DR) was determined from the CO_2 concentrations measured at
205 the stack, diluted stack, and background, where:

$$206 \quad DR = \frac{CO_{2,Stk} - CO_{2,Bkg}}{CO_{2,Dil} - CO_{2,Bkg}}$$

207 where $CO_{2,Stk}$ is the CO_2 concentration in the stack; $CO_{2,Bkg}$ the background CO_2
208 concentration in the atmosphere; and $CO_{2,Dil}$ the CO_2 concentration in the diluted
209 smoke.

210 **2.4. Stable carbon isotope composition of diacids**

211 Stable carbon isotopic determinations ($\delta^{13}C$) of diacids, ketocarboxylic acids,
212 and α -dicarbonyls followed the techniques of Kawamura and Watanabe (2004). The
213 isotope values of the derivatized samples were determined using a gas
214 chromatography–isotope ratio mass spectrometer (GCIR-MS; Thermo Fisher, Delta V
215 Advantage, Franklin, MA, USA). The $\delta^{13}C$ values were then calculated for free
216 organic acids using an isotope mass balance equation based on the measured $\delta^{13}C$
217 values of derivatives and BF_3/n -butanol (Kawamura and Watanabe, 2004). To ensure
218 the analytical error of the $\delta^{13}C$ values less than 0.2‰, each aerosol sample was
219 analyzed in triplicate, to obtain the average values.

220 **3. Results and Discussion**

221 **3.1. Emission factors for diacids, ketocarboxylic acids, α -dicarbonyls**

222 Fresh and aged $PM_{2.5}$ EFs for a homologous series of diacids, ketocarboxylic
223 acids (glyoxylic acid, ωC_2 and pyruvic acid, Pyr), α -dicarbonyls (glyoxal, Gly and
224 methylglyoxal, mGly) and benzoic acid are presented in Table 1. The EFs for most
225 fresh and aged diacids varied by severely order-of-magnitude with higher EFs after
226 atmospheric aging. The highest fresh EF (i.e. EF_{fresh}) was found for wheat straw

227 ranging 44-122 mg kg⁻¹ for succinic acid (C₄) and 67-102 mg kg⁻¹ for Gly, higher than
228 those found in maize and rice. The arithmetic means and standard deviations for the
229 EF_{fresh} of total diacids from burning of rice, maize, and wheat straws were 63 ± 24,
230 117 ± 39, and 285 ± 135 mg kg⁻¹, respectively.

231 As is shown Fig. 1, distributions of diacids in fresh emissions varied by crop
232 types and species. Of the saturated n-dicarboxylic acids, C₄ acid was the most
233 abundant species in the maize and wheat straw with average EF_{fresh} of 22 ± 12 and 83
234 ± 46 mg kg⁻¹, respectively. Azelaic acid (C₉) and C₄ were the most abundant species
235 from rice burning with EF_{fresh} of 11 ± 2.9 and 10 ± 9.0 mg kg⁻¹, respectively. These
236 findings are consistent with the fresh smoke aerosols in Siberian BB plumes
237 (Kalogridis et al., 2018), in which C₄ and C₉ were more abundant than C₂. Previous
238 studies also showed C₉ to be an oxidation product of unsaturated fatty acids in
239 biomass smoke (Kawamura and Gagosian, 1987; Kawamura et al., 2013; Agarwal et
240 al., 2010; Cao et al., 2017). C₂ is the most abundant species of diacids and is one of
241 the final products of SOA reaction chain. In the fresh BB sample, C₂ emissions were
242 lower due to the short aging time.

243 Similar to the diacids, the highest EF_{fresh} for ketocarboxylic acids and
244 α-dicarbonyls were also found in wheat straw samples, with 44 ± 31 and 138 ± 91 mg
245 kg⁻¹, respectively. Gly was the highest α-dicarbonyls, with average EF_{fresh} of 27 ± 3.9,
246 42 ± 10, and 84 ± 41 mg kg⁻¹ for rice, maize and wheat straw, respectively. This is
247 consistent with previous studies which showed that Gly is often more abundant than
248 mGly in polluted aerosols collected from China (Pavuluri et al., 2010; Ho et al., 2007).
249 Benzoic acid also was determined, and its EF_{fresh} for rice, maize, and wheat aerosols
250 were 1.9 ± 0.2, 2.5 ± 0.4, and 3.1 ± 0.3 mg kg⁻¹ (Table 1).

251 **3.2. Effects of atmospheric aging processes**

252 3.2.1 Diacids

253 The EF_{aged} of 2- and 7-day diacids were 1650 ± 438 and 1957 ± 598 mg/kg,
254 respectively (Table S1); approximately 10 times greater than the EF_{fresh}. High
255 aged/fresh (A/F) ratios implies that the bulk of the total diacids were secondarily
256 produced through aging processes. Longer exposure time in the atmosphere increased

257 the formation of diacids as ratios of average A/F increased from 9.1 (2-day) to 10.8
258 (7-day) (Table S1). As shown in Fig. 2, C₂ was the most abundant of all measured
259 diacids among three crops, with the highest EF_{aged} found in wheat (1412 ± 328 mg/kg)
260 after 7-day aging. These results provide further evidence that C₂ is produced mainly
261 through secondary photochemical processes rather than direct emission from BB. That
262 is one possible reason why C₂ is often the most abundant diacid in ambient samples,
263 especially in the oceanic and other remote areas (Hoque et al., 2020; Kawamura and
264 Usukura, 1993; Kawamura and Sakaguchi, 1999; Kunwar and Kawamura, 2014; Hegde
265 and Kawamura, 2012; Kawamura and Bikkina, 2016; Wang et al., 2012). In addition,
266 we found that the A/F ratio of C₂ after 2-day aging was 50.8, and the change from 2~
267 to 7 day was relatively small, only increasing by 13.7 (Table S1). These results meant
268 that 2-day aging may be sufficient for most diacids formation. It can be inferred that
269 although diacids is still generated at 7-day aging, a large number of VOCs may have
270 been oxidized at 2-day aging and transferred to the particle phase by condensation,
271 adsorption and other ways. Especially for maize straw, the EF_{aged} of total detected
272 organics at 7-day aging (1844 ± 344 mg/kg) was lower than that of at 2-day aging
273 (3530 ± 626 mg/kg), which was mainly due to predominant role of particulate diacids
274 degradation in longer aging time. This phenomenon is consistent with the change of
275 EF_S of VOCs (precursors of C₂) during maize straw combustion. The decreases in of
276 ΣVOC_{EF} after 2-day aging (1227 mg/kg) were comparable with those of 7-day aging
277 (884 mg/kg) for maize straw (Niu et al., 2020).

278 C₄ ranked second in abundance after C₂, with 7-8 folds increased in EF after 2-
279 and 7-day aging wheat. Although malonic acid (C₃) is mainly produced by the
280 photochemical oxidation of C₄, it also can be formed through the incomplete
281 combustion of fossil fuels and biomass (Kawamura and Ikushima, 1993). In the
282 atmosphere, C₄ is typically more abundant than C₃ originated from BB, vehicular
283 engine exhaust and biogenic emissions (Fu et al., 2013; Kawamura and Kaplan, 1987;
284 Kundu et al., 2010). Fig. 3 shows atmospheric aging increased the abundances of C₃
285 and C₄ with A/F ratios increased from 16.2 to 31.1 for C₃, and from 5.7 to 8.0 in C₄
286 from 2- to 7-day of aging (Table S1). These findings add to the evidence that these

287 diacids are produced by the photo-oxidation of primary pollutants emitted from
288 combustion process. Higher A/F ratios in aged and fresh C₃ acid than those of C₄ acid
289 may be attributed to rapid formation rate of C₃ or decarboxylation processing of C₄
290 diacid during aging (Zhao et al., 2018).

291 As mentioned above, C₉ is thought to be mainly formed through the
292 photochemical oxidation of unsaturated fatty acids emitted by plants (Kawamura and
293 Gagosian, 1987). Average EFs in C₉ acid were low, ranging from 18 ± 7.3 mg kg⁻¹
294 (fresh), to 51 ± 14 mg kg⁻¹ (2-day), with A/F ratios of C₉ of 2.8, and 2.2 for the 2- and
295 7-day samples, respectively, suggesting that C₉ is relatively stable with short
296 residence time. Fig.3 shows that A/F ratios of other long-chain diacids and branched
297 diacids did not show apparent changes between the 2- and 7-day samples, which may
298 be due to the degradation of long-chain diacids (Enami et al., 2015;Legrand et al.,
299 2007;Miyazaki et al., 2010). It is also possible that the laboratory combustion
300 experiment did not produce adequate quantities of certain diacids. For example,
301 glutaric acid (C₅) and adipic acid (C₆) are commonly formed by reactions of
302 cycloolefins emitted from anthropogenic sources with O₃ (Hatakeyama et al., 1985),
303 and phthalic acid as a product of the photochemical oxidation of aromatic
304 hydrocarbon compounds (Kawamura and Ikushima, 1993). Additional laboratory
305 experiments may be needed to reify different atmospheric process.

306 3.2.2 Ketocarboxylic acids and α-carbonyls

307 In contrast to the diacids, aging process were not apparent in ketocarboxylic
308 acids as A/F ratios reduced by 16% from 13.8 (2-day) to 11.9 (7-day). Similar
309 phenomenon was found for α-carbonyls with A/F ratios reduced by 64% from 5.4
310 (2-day) to 3.3 (7-day). This suggests the possibility that the degradation of these
311 intermediates to C₂ is faster than their formation by oxidation after 2 days of aging.
312 Fig.3 also show apparent reduction EF of 33-42% from 2- to 7-day aging for Gly and
313 mGly which may be due to the fact both Gly and mGly initially can be oxidized to
314 less volatile polar organic acids including Pyr and ωC₂ and then further oxidized to C₂
315 (Wang et al., 2012;Warneck, 2003).

316 **3.3. Comparisons of diagnostic ratios of diacids in fresh and aged aerosols**

317 Patterns in the relative abundances of diacids have been used to evaluate
318 biogenic versus anthropogenic source strengths and the photochemical processing of
319 organic aerosols (Kawamura et al., 2012). Previous studies have shown that C₄ can be
320 directly oxidized into C₂ or via C₃ into C₂ (Jung et al., 2010; Sorooshian et al., 2007),
321 with C₂ being an end-product of the photochemical oxidation (Wang et al., 2012). The
322 ratios of C₃/C₄, C₂/C₄ and C₂/total diacids can be regarded as indicators of aerosol
323 aging (Cheng et al., 2013; Kunwar et al., 2019; Meng et al., 2018; Pavuluri et al.,
324 2010), with higher ratios indicative of more aged aerosols (Kawamura and Sakaguchi,
325 1999). As shown in Table 2, the ratios in this study showed a clear atmospheric aging
326 trend from fresh to 7-day aging with ratios of 0.7 to 6.4 for C₂/C₄, 0.1 to 0.6 in
327 C₂/total diacids and 0.2 to 0.5 in C₃/C₄, indicating obvious photochemical oxidation.

328 Ratios of ωC₂/C₂ and Gly/mGly can also be used to evaluate the oxidation of
329 organic aerosols (Cheng et al., 2013, 2015; Kawamura et al., 2013). In the study,
330 apparent reduction of the ωC₂/C₂ ratios from 1.3 (fresh) to 0.2 (7-day) supports the
331 potential oxidation pathways from precursor glyoxylic to oxalic acids. Aqueous-phase
332 oxidation by OH is faster for Gly than for mGly, and the abundance of Gly relative to
333 mGly is an indicator of aerosol aging (Cheng et al., 2013). The ratio of Gly/mGly in
334 xi'an samples was lower in haze days than in clean days, and lower in summer than in
335 winter. Similarly, the Gly/mGly ratios in the aged BB samples were higher in the
336 fresh PM_{2.5} samples (3.8) compared to the 2-day (2.3) and 7-day (2.0) aging.

337 Ratios of C₃/C₄, C₂/diacids, ωC₂/C₂, and Gly/mGly are similar among studies.
338 Except for the higher C₃/C₄ ratio of 3.9 found in marine aerosols of over the pacific
339 region (Kawamura and Sakaguchi, 1999), and lower C₃/C₄ ratios in Siberian BB
340 emissions in a large aerosol chamber (<0.03) (Kalogridis et al., 2018). The largest
341 difference was found for C₂/C₄, varied from <1 for fresh aerosol in Siberian BB
342 (Kalogridis et al., 2018), to 25.2 from forest fire in Thailand (Boreddy et al., 2020).
343 Elevated C₂/C₄ ratios exceeding 10 were found in aged ambient Xi'an, China (10.4)
344 (Cheng et al., 2013), Mt. Hua, China (10.7) (Meng et al., 2014), marine aerosol,
345 Pacific ocean (14.3) (Kawamura and Sakaguchi, 1999), and ambient island Okinawa,

346 Japan (15.5) (Kunwar and Kawamura, 2014). These C₂/C₄ ratios are ~63% to 142%
347 higher than these reported in this study. Overall, these comparisons show the
348 importance of photochemical aging, however, the atmospheric oxidation evidently
349 was more extensive in aerosols from some remote mountain and marine
350 environments.

351 **3.4. Stable carbon isotopes of diacids**

352 Stable carbon isotope ratios ($\delta^{13}\text{C}$) can provide insights into the sources of
353 aerosols, Pavuluri and Kawamura (2016) reported that average $\delta^{13}\text{C}$ values for C₂
354 from biogenic aerosols (-15.8‰) were less negative—i.e., contained more ¹³C and
355 was isotopically enriched than those from anthropogenic aerosols (-19.5‰). Data for
356 $\delta^{13}\text{C}$ also can provide information on the processing or aging of organic aerosols
357 because isotopic fractionation result from chemical reactions or phase transfer
358 (Pavuluri and Kawamura, 2016; Zhang et al., 2016). Mass loading of $\delta^{13}\text{C}$ for diacids
359 in the fresh BB samples were too low to be detected by the GCIR-MS, but the $\delta^{13}\text{C}$
360 values for C₂ ranged from -23.3 to -21.0 ‰ (with an average of -21.9 ± 1.2 ‰) in
361 2-day and -19.1 to -15.5 ‰ (-17.3 ± 1.7 ‰) for 7-day aged samples (Table 3).

362 Table 3 shows that the average $\delta^{13}\text{C}$ values of C₂ from aged maize samples
363 higher than those of rice and wheat. The reason for the isotope difference may be that
364 maize is a C₄ plant, while wheat and rice are both C₃ plants. Song et al. (2018)
365 showed that $\delta^{13}\text{C}_{\text{TC}}$ in C₄ plants is isotopically heavier than in C₃ plants. Moreover,
366 the $\delta^{13}\text{C}$ of C₂ is more abundant in 7- than 2-day samples (Table 3) with -13.1 ± 1.6 ‰
367 (2-day) and -7.1 ± 1.4 ‰ (7-day) in maize; -26.2 ± 1.8 ‰ (2-day) and -20.8 ± 3.3 ‰
368 (7-day) in rice and -26.5 ± 0.2 ‰ (2-day) and -24.0 ± 0.5 ‰ (7-day) in wheat
369 combustion. The $\delta^{13}\text{C}$ data for C₃, C₄ and ωC_2 (Table S2) showed similar trends,
370 consistent with previous studies. For example, Zhao et al. (2018) found that the $\delta^{13}\text{C}$
371 values of C₂ were related to aging. Pavuluri and Kawamura (2016) analyzed diacids,
372 ωC_2 , and Gly for $\delta^{13}\text{C}$ in anthropogenic and biogenic aerosol samples by UV
373 irradiation, and reported more $\delta^{13}\text{C}$ less negative with longer irradiation times. During
374 atmospheric oxidation reactions, organic compounds react with OH radicals, causing
375 the release of CO₂ and CO which contain relatively the lighter ¹²C isotope and thus

376 leaving the remaining substrate enriched in ^{13}C (Hoefs, 1997; Sakugawa and Kaplan,
377 1995).

378 A comparison of $\delta^{13}\text{C}$ values for C_2 in the aerosols from selected environments is
379 shown in Fig. 4. Average $\delta^{13}\text{C}$ value ($-21.9 \pm 1.2 \text{‰}$) of 2-day aged biomass burning
380 of C_2 was comparable to those reported for urban regions, such as Beijing ($-21.8 \pm$
381 2.8‰) (Zhao et al., 2018) and Liaocheng ($-19.8 \pm 3.1\text{‰}$) (Meng et al., 2020) (Table 3).
382 With continued aging, the C_2 $\delta^{13}\text{C}$ of the 7-day samples ($-17.3 \pm 1.7 \text{‰}$) was more
383 similar in samples from Mt. Tai ($-16.5 \pm 1.8\text{‰}$) (Meng et al., 2018) and western
384 Pacific and Southern Ocean aerosol ($-16.8 \pm 0.8\text{‰}$) (Wang and Kawamura, 2006), but
385 it was significantly lighter than that of samples from the Korea Climate Observatory
386 at Gosan ($-13.7 \pm 2.5\text{‰}$), which is a mountain background site in East Asia (Zhang et
387 al., 2016).

388 **3.5. Relationships between decreases VOCs and increases diacids**

389 During the chamber experiment (Niu et al., 2020) concerning measured the VOC
390 compounds. Table S3 presents the correlations between decreases in VOCs and
391 increases in diacids from fresh to 2-day aged BB samples. Significant ($0.01 < p < 0.05$)
392 correlations (R) were observed for toluene with Gly (R = 0.75), mGly (R = 0.81), Pyr
393 (R = 0.78), ωC_2 (R = 0.78) and C_2 (R = 0.67) (Fig. 5), suggesting that toluene was
394 converted to diacids during the aging processes. Indeed, it has been reported that the
395 photooxidation of toluene is a potential source of secondary organic aerosol (SOA) in
396 urban air (Sato et al., 2007), and the major chemical components of the SOA include
397 hemiacetal, peroxy hemiacetal oligomers and diacids. It also can be seen that benzene
398 had significant correlations with mGly and C_2 ($R > 0.59$ in Fig.5), implying that the
399 oxidation of benzene led to diacid formation. Photooxidation of Gly and mGly is a
400 major global and regional source of C_2 diacid, and the two formation pathways
401 are Gly- ωC_2 - C_2 and mGly-Pyr- ωC_2 - C_2 , respectively (Yasmeen et al., 2010; Wang et
402 al., 2012). As shown in the Fig.5, the slope (0.20~0.59) between the decrease of
403 toluene and the increase of intermediates (Gly, mGly, Pyr and ωC_2) is significantly
404 higher than C_2 (0.04). Same thing with benzene, the slope between decrease of
405 benzene and increase of mGly is 0.55, while C_2 is only 0.05.

406 On the global scale isoprene is the most important precursor for C₂, contributing
407 70% to the global C₂, while anthropogenic VOCs contribute 21% to C₂ production
408 (Myriokefalitakis et al., 2011). Thus, it is not surprising that isoprene correlated with
409 C₂ (R=0.58) (Fig.5). In addition, several alkenes and alkanes also had a significant
410 correlation with C₂ (Table S3), indicating that these species may react in secondary
411 oxidation processes to generate C₂. Previous studies have confirmed that diacids can
412 be oxidation products of aromatic hydrocarbons (Borrás and Tortajada-Genaro, 2012),
413 cycloolefins (Hamilton et al., 2006), and may originated from diesel vehicle exhaust
414 (Samy and Zielinska, 2010). However, no significant correlation was found between
415 decreases in VOCs and increases in 7-day aged diacids. For the longer aging times,
416 the particulate phase compounds may be further oxidized to generate other
417 compounds besides diacids. Such a correlation between decreases VOCs and
418 increases diacids again suggests that 2-day aging may be sufficient to oxidize VOCs
419 to diacids.

420 **4. Conclusions**

421 The emission factors (EFs) of dicarboxylic acids (diacids) and related
422 compounds in experimentally produced fresh and aged biomass burning (BB) aerosols
423 were compared. For fresh emissions, succinic acid (C₄) was the most abundant diacid
424 species followed by azelaic acid (C₉). After atmospheric aging, diacids was dominated
425 by oxalic acid (C₂), with elevated EFs. Ratios of aged to fresh (A/F) for C₂ increased
426 from 50.8 (2-day) to 64.5 (7-day). These results suggest that the diacids in the
427 atmosphere largely originated from secondary photochemical processes as opposed to
428 primary emissions from BB. It is confirmed for the first time whether the contribution
429 of BB source to diacids is formed by primary emission or secondary oxidation. In
430 addition, by comparing the EFs and A/F ratio of 2-day and 7-day aging, it was found
431 that 2 days of aging is sufficient for many diacids. Moreover, the 2-day A/F ratios 2.8
432 of azelaic acid (C₉) degraded by 27% after 7-days, suggesting that this species is
433 relatively stable with short residence time.

434 Decreasing trends in EFs were found for ketocarboxylic acids and α -dicarbonyls,
435 from 2-day to 7-day aging with A/F ratios reduced from 13.8 to 11.9 and from 5.4 to
436 3.3, respectively. These results suggest that after 2-day aging, the net degradation of
437 these intermediates was faster than their rates of formation. Compared with 2-day
438 samples, the $\delta^{13}\text{C}$ of C_2 , malonic acid (C_3), C_4 and glyoxylic acid (ωC_2) in 7-day
439 samples became more positive or isotopically heavier after the additional aging, likely
440 due to kinetic isotope fractionation effects. Moreover, the $\delta^{13}\text{C}$ values for the aged
441 maize samples in both the 2- and 7-day samples were significantly more positive than
442 those of rice and wheat. This may be due to their different plant types with maize
443 being a C_4 plant while wheat and rice are both C_3 plants. The correlations between
444 volatile organic compounds (VOCs) and C_2 or intermediates indicated that the
445 oxidation of VOCs led to the formation of diacids. This correlation exists only at
446 2-day aging, but does not exist at 7-day aging, probably because the longer the aging
447 time, the particle phase compounds may be further oxidized to other compounds.

448 Diacid are highly water-soluble in nature and thus their high abundances due to
449 BB and intense photochemical aging would enhance the ability of aerosols to act as
450 cloud condensation nuclei and modify the water-uptake properties of aerosol
451 particles. Therefore, it is necessary to better understand the chemical and physical
452 properties of the constituents of water-soluble organic smoke, as they may have a
453 significant impact on climate forcings through indirect aerosol effects. The results
454 provide in-depth understanding of secondary organic aerosol (SOAs) formation in
455 regions greatly affected by BB.

456 **Data availability**

457 The data involved in this study will be provided when they are asked from the
458 corresponding authors.

459 **Author contribution**

460 Junji Cao and Jianjun Li conceived and designed the study. Minxia Shen
461 contributed to the literature search, samples and data analysis, and manuscript writing.
462 Jianjun Li, Junji Cao, Judith C. Chow and John G. Watson contributed to manuscript

463 revision. Kin Fai Ho, Wenting Dai, Suixin Liu, Ting Zhang, Qiyuan Wang, Jingjing
464 Meng carried out the particulate samples and supervised the experiments. All authors
465 commented on the manuscript and reviewed the manuscript.

466 **Declaration of Competing Interest**

467 The authors declare that they have no known competing financial interests or
468 personal relationships that could have appeared to influence the work reported in this
469 paper.

470 **Acknowledgments**

471 This work was jointly supported by the program from National Nature Science
472 Foundation of China (No. 41977332), the Strategic Priority Research Program of
473 Chinese Academy of Sciences (No. XDB40000000), the Innovation Capability
474 Support Program of Shaanxi (No. 2020KJXX-017), and by the US National Science
475 Foundation (AGS-1464501 and CHE 1214463). Jianjun Li also acknowledges the
476 support of the Youth Innovation Promotion Association CAS (No. 2020407).

477 **References**

- 478 Agarwal, S., Aggarwal, S. G., Okuzawa, K., and Kawamura, K.: Size distributions of dicarboxylic
479 acids, ketoacids, α -dicarbonyls, sugars, WSOC, OC, EC and inorganic ions in atmospheric particles
480 over Northern Japan: implication for long-range transport of Siberian biomass burning and East Asian
481 polluted aerosols, *Atmos. Chem. Phys.*, 10, 5839-5858, <https://doi.org/10.5194/acp-10-5839-2010>,
482 2010.
- 483 Aggarwal, S. G., Kawamura K.: Molecular distributions and stable carbon isotopic compositions
484 of dicarboxylic acids and related compounds in aerosols from Sapporo, Japan: Implications for
485 photochemical aging during long-range atmospheric transport, *J. Geophys. Res.*, 113, D14301,
486 <https://doi.org/10.1029/2007JD009365>, 2008
- 487 Akagi, S. K., Yokelson, R. J., Wiedinmyer, C., Alvarado, M. J., Reid, J. S., Karl, T., Crouse, J. D., and
488 Wennberg, P. O.: Emission factors for open and domestic biomass burning for use in atmospheric
489 models, *Atmos. Chem. Phys.*, 11, 4039-4072, <https://doi.org/10.5194/acp-11-4039-2011>, 2011.
- 490 Andreae, M. O., and Merlet, P.: Emission of trace gases and aerosols from biomass burning, *Global*
491 *Biogeochem. Cy.*, 15, 955-966, <https://doi.org/10.1029/2000GB001382>, 2001.
- 492 Bikkina, S., Kawamura, K., Sakamoto, Y., and Hirokawa, J.: Low molecular weight dicarboxylic acids,
493 oxocarboxylic acids and α -dicarbonyls as ozonolysis products of isoprene: Implication for the
494 gaseous-phase formation of secondary organic aerosols, *Sci. Total Environ.*, 769, 14472,
495 <https://doi.org/10.1016/j.scitotenv.2020.144472>, 2021.
- 496 Boreddy, S. K. R., Parvin, F., Kawamura, K., Zhu, C. M., and Lee, C. T.: Influence of forest fires on the
497 formation processes of low molecular weight dicarboxylic acids, ω -oxocarboxylic acids, pyruvic acid
498 and α -dicarbonyls in springtime fine (PM_{2.5}) aerosols over Southeast Asia, *Atmos. Environ.*, 246,
499 118065, <https://doi.org/10.1016/j.atmosenv.2020.118065>, 2020.
- 500 Borrás, E., and Tortajada-Genaro, L. A.: Secondary organic aerosol formation from the photo-oxidation
501 of benzene, *Atmos. Environ.*, 47, 154-163, <https://doi.org/10.1016/j.atmosenv.2011.11.020>, 2012.
- 502 Cao, F., Zhang, S. C., Kawamura, K., Liu, X. Y., Yang, C., Xu, Z. F., Fan, M. Y., Zhang, W. Q., Bao, M.
503 Y., Chang, Y. H., Song, W. H., Liu, S. D., Lee, X. H., Li, J., Zhang, G., and Zhang, Y. L.: Chemical
504 characteristics of dicarboxylic acids and related organic compounds in PM_{2.5} during biomass-burning
505 and non-biomass-burning seasons at a rural site of Northeast China, *Environ. Pollut.*, 231, 654-662,
506 <https://doi.org/10.1016/j.envpol.2017.08.045>, 2017.
- 507 Cao, J. J., Wang, Q. Y., Li, L., Zhang, Y., Tian, J., Chen, L. W. A., Ho, S. S. H., Wang, X. L., Chow, J.
508 C., and Watson, J. G.: Evaluation of the oxidation flow reactor for particulate matter emission limit
509 certification, *Atmos. Environ.*, 224, <https://doi.org/10.1016/j.atmosenv.2019.117086>, 2020.
- 510 Carlton, A. G., Turpin, B. J., Lim, H. J., Altieri, K. E., and Seitzinger, S.: Link between isoprene and
511 secondary organic aerosol (SOA): Pyruvic acid oxidation yields low volatility organic acids in clouds,
512 *Geophys. Res. Lett.*, 33, L06822, <https://doi.org/10.1029/2005GL025374>, 2006.
- 513 Carlton, A. G., Turpin, B. J., Altieri, K. E., Seitzinger, S., Reff, A., Lim, H. J., and Ervens, B.:
514 Atmospheric oxalic acid and SOA production from glyoxal: Results of aqueous photooxidation
515 experiments, *Atmos. Environ.*, 41, 7588-7602, <https://doi.org/10.1016/j.atmosenv.2007.05.035>, 2007.
- 516 Chen, J. M., Li, C. L., Ristovski, Z., Milic, A., Gu, Y. T., Islam, M. S., Wang, S. X., Hao, J. M., Zhang,
517 H. F., He, C. R., Guo, H., Fu, H. B., Miljevic, B., Morawska, L., Thai, P., Fat LAM, Y., Pereira, G.,
518 Ding, A. J., Huang, X., and Dumka, U. C.: A review of biomass burning: Emissions and impacts on air
519 quality, health and climate in China, *Sci. Total Environ.*, 579, 1000-1034,

520 <https://doi.org/10.1016/j.scitotenv.2016.11.025>, 2016.

521 Cheng, C. L., Wang, G. H., Zhou, B. H., Meng, J. J., Li, J. J., and Cao, J. J.: Comparison of
522 dicarboxylic acids and related compounds in aerosol samples collected in Xi'an, China during haze and
523 clean periods, *Atmos. Environ.*, 81, 443-449, <https://doi.org/10.1016/j.atmosenv.2013.09.013>, 2013.

524 Cheng, C. L., Wang, G. H., Meng, J. J., Wang, Q. Y., Cao, J. J., Li, J. J., and Wang, J. Y.: Size-resolved
525 airborne particulate oxalic and related secondary organic aerosol species in the urban atmosphere of
526 Chengdu, China, *Atmos. Res.*, 161-162, 134-142, <https://doi.org/10.1016/j.atmosres.2015.04.010>, 2015.

527 Chow, J. C., Cao, J. J., Antony Chen, L. W., Wang, X. L., Wang, Q. Y., Tian, J., Ho, S. S. H., Watts, A.
528 C., Carlson, T. B., Kohl, S. D., and Watson, J. G.: Changes in PM_{2.5} peat combustion source profiles
529 with atmospheric aging in an oxidation flow reactor, *Atmos. Meas. Tech.*, 12, 5475-5501,
530 <https://doi.org/10.5194/amt-12-5475-2019>, 2019.

531 Enami, S., Hoffmann, M. R., and Colussi, A. J.: Stepwise Oxidation of Aqueous Dicarboxylic Acids by
532 Gas-Phase OH Radicals, *J. Phys. Chem. Lett.*, 6, 527-534, <https://doi.org/10.1021/jz502432j>, 2015.

533 FaLkovich, A. H., Graber, E. R., Schkolnik, G., Rudich, Y., Maenhaut, W., and Artaxo, P.: Low
534 molecular weight organic acids in aerosol particles from Rondônia, Brazil, during the biomass-burning,
535 transition and wet periods, *Atmos. Chem. Phys.*, 5, 781-797, <https://doi.org/10.5194/acp-5-781-2005>,
536 2005.

537 Fu, P. Q., Kawamura, K., Usukura, K., and Miura, K.: Dicarboxylic acids, ketocarboxylic acids and
538 glyoxal in the marine aerosols collected during a round-the-world cruise, *Mar. Chem.*, 148, 22-32,
539 <https://doi.org/10.1016/j.marchem.2012.11.002>, 2013.

540 Fullerton, D. G., Nigel, B., and Gordon, S. B.: Indoor air pollution from biomass fuel smoke is a major
541 health concern in the developing world, *T. Roy. Soc. Trop. Med. H.*, 102, 843-851,
542 <https://doi.org/10.1016/j.trstmh.2008.05.028>, 2008.

543 Gilman, J. B., Lerner, B. M., Kuster, W. C., Goldan, P. D., Warneke, C., Veres, P. R., Roberts, J. M., de
544 Gouw, J. A., Burling, I. R., and Yokelson, R. J.: Biomass burning emissions and potential air quality
545 impacts of volatile organic compounds and other trace gases from fuels common in the United States.,
546 *Atmos. Chem. Phys.*, 15, 13915-13938, <https://doi.org/10.5194/acp-15-13915-2015>, 2015.

547 Hamilton, J. F., Lewis, A. C., Reynolds, J. C., Carpenter, L. J., and Lubben, A.: Investigating the
548 composition of organic aerosol resulting from cyclohexene ozonolysis: low molecular weight and
549 heterogeneous reaction products, *Atmos. Chem. Phys.*, 6, 4973-4984,
550 <https://doi.org/10.5194/acpd-6-6369-2006>, 2006.

551 Hatakeyama, S., Tanonaka, T., Weng, J., Bandow, H., Takagi, H., and Akimoto, H.: Ozone-cyclohexene
552 reaction in air: quantitative analysis of particulate products and the reaction mechanism, *Environ. Sci.*
553 *Technol.*, 19, 935-942, <https://doi.org/10.1021/es00140a008>, 1985.

554 Hegde, P., and Kawamura, K.: Seasonal variations of water-soluble organic carbon, dicarboxylic acids,
555 ketocarboxylic acids, and α -dicarbonyls in Central Himalayan aerosols, *Atmos. Chem. Phys.*, , 12,
556 6645-6665, <https://doi.org/10.5194/acp-12-6645-2012>, 2012.

557 Ho, K. F., Lee, S. C., Cao, J. J., Kawamura, K., Watanabe, T., Cheng, Y., and Chow, J. C.: Dicarboxylic
558 acids, ketocarboxylic acids and dicarbonyls in the urban roadside area of Hong Kong, *Atmos. Environ.*,
559 40, 3030-3040, <https://doi.org/10.1016/j.atmosenv.2005.11.069>, 2006.

560 Ho, K. F., Cao, J. J., Lee, S. C., Kawamura, K., Zhang, R. J., Chow, J. C., and Watson, J. G.:
561 Dicarboxylic acids, ketocarboxylic acids, and dicarbonyls in the urban atmosphere of China, *J.*
562 *Geophys. Res.-Atmos.*, 112, D22S27, <https://doi.org/10.1029/2006JD008011>, 2007.

563 Hodshire, A. L., Akherati, A., Alvarado, M. J., Brown-Steiner, B., Jathar, S. H., Jimenez, J. L.,

564 Kreidenweis, S. M., Lonsdale, C. R., Onasch, T. B., Ortega, A. M., and Pierce, J. R.: Aging effects on
565 biomass burning aerosol mass and composition: a critical review of field and laboratory studies,
566 *Environ. Sci. Technol.*, 53, 10007-10022, <https://doi.org/10.1021/acs.est.9b02588>, 2019.

567 Hoefs, J.: *Stable Isotope Geochemistry*, 1997.

568 Hoque, M., Kawamura, K., Nagayama, T., Kunwar, B., and Gagosian, R. B.: Molecular characteristics
569 of water-soluble dicarboxylic acids, ω -oxocarboxylic acids, pyruvic acid and α -dicarbonyls in the
570 aerosols from the eastern North Pacific, *Mar. Chem.*, 224,
571 <https://doi.org/10.1016/j.marchem.2020.103812>, 2020.

572 Jung, J. S., Tsatsral, B., Kim, Y. J., and Kawamura, K.: Organic and inorganic aerosol compositions in
573 Ulaanbaatar, Mongolia, during the cold winter of 2007 to 2008 : Dicarboxylic acids, ketocarboxylic
574 acids, and α -dicarbonyls, *J. Geophys. Res.-Atmos.*, 115, D22203,
575 <https://doi.org/10.1029/2010JD014339>, 2010.

576 Kalogridis, A. C., Popovicheva, O. B., Engling, G., Diapouli, E., Kawamura, K., Tachibana, E., Ono,
577 K., Kozlov, V. S., and Eleftheriadis, K.: Smoke aerosol chemistry and aging of Siberian biomass
578 burning emissions in a large aerosol chamber, *Atmos. Environ.*, 185, 15-28,
579 <https://doi.org/10.1016/j.atmosenv.2018.04.033>, 2018.

580 Kang, E., Root, M., Toohey, D., and Brune, W.: Introducing the concept of Potential Aerosol Mass
581 (PAM), *Atmos. Chem. Phys.*, 7, 5727-5744, <https://doi.org/10.5194/acp-7-5727-2007>, 2007.

582 Kawamura, and Usukura, K.: Distributions of low molecular weight dicarboxylic acids in the North
583 Pacific aerosol samples, *J. Oceanogr.*, 49, 271-283, <https://doi.org/10.1007/BF02269565>, 1993.

584 Kawamura, K., and Gagosian, R. B.: Implications of ω -oxocarboxylic acids in the remote marine
585 atmosphere for photo-oxidation of unsaturated fatty acids, *Nature* 325, 330-332, 1987.

586 Kawamura, K., and Kaplan, I. R.: Motor exhaust emissions as a primary source for dicarboxylic acids
587 in Los Angeles ambient air, *Environ. Sci. Technol.*, 21, 105-110, <https://doi.org/10.1021/es00155a014>,
588 1987.

589 Kawamura, K., and Ikushima, K.: Seasonal changes in the distribution of dicarboxylic acids in the
590 urban atmosphere, *Environ. Sci. Technol.*, 27, 2227-2235, <https://doi.org/10.1021/es00047a033>, 1993.

591 Kawamura, K., Kasukabe, H., and Barrie, L. A.: Source and reaction pathways of dicarboxylic acids,
592 ketoacids and dicarbonyls in arctic aerosols: one year of observations, *Atmos. Environ.*, 30, 1709-1722,
593 [https://doi.org/10.1016/1352-2310\(95\)00395-9](https://doi.org/10.1016/1352-2310(95)00395-9), 1996a.

594 Kawamura, K., Sempéré, R., Imai, Y., Fujii, Y., and Hayashi, M.: Water soluble dicarboxylic acids and
595 related compounds in Antarctic aerosols, *J. Geophys. Res.-Atmos.*, 101, 18721-18728,
596 <https://doi.org/10.1029/96JD01541>, 1996b.

597 Kawamura, K., and Sakaguchi, F.: Molecular distributions of water soluble dicarboxylic acids in
598 marine aerosols over the Pacific Ocean including tropics, *J. Geophys. Res.-Atmos.*, 104, 3501-3509,
599 <https://doi.org/10.1029/1998JD100041>, 1999.

600 Kawamura, K., Yokoyama, K., Fujii, Y., and Watanabe, O.: A Greenland ice core record of low
601 molecular weight dicarboxylic acids, ketocarboxylic acids, and α -dicarbonyls: A trend from Little Ice
602 Age to the present (1540 to 1989 A.D.), *J. Geophys. Res.-Atmos.*, 106, 1331-1345,
603 <https://doi.org/10.1029/2000JD900465>, 2001.

604 Kawamura, K., and Watanabe, T.: Determination of stable carbon isotopic compositions of low
605 molecular weight dicarboxylic acids and ketocarboxylic acids in atmospheric aerosol and snow samples,
606 *Anal. Chem.*, 76, 5762-5768, <https://doi.org/10.1021/ac049491m>, 2004.

607 Kawamura, K., Ono, K., Tachibana, E., Charriere, B., and Sempere, R.: Distributions of low molecular

608 weight dicarboxylic acids, ketoacids and α -dicarbonyls in the marine aerosols collected over the Arctic
609 Ocean during late summer, *Biogeosciences*, 9, 4725-4737, <https://doi.org/10.5194/bg-9-4725-2012>,
610 2012.

611 Kawamura, K., Tachibana, E., Okuzawa, K., Aggarwal, S. G., Kanaya, Y., and Wang, Z. F.: High
612 abundances of water-soluble dicarboxylic acids, ketocarboxylic acids and α -dicarbonyls in the
613 mountaintop aerosols over the North China Plain during wheat burning season, *Atmos. Chem. Phys.*,
614 13, 8285-8302, <https://doi.org/10.5194/acp-13-8285-2013>, 2013.

615 Kawamura, K., and Bikkina, S.: A review of dicarboxylic acids and related compounds in atmospheric
616 aerosols: Molecular distributions, sources and transformation, *Atmos. Res.*, 170, 140-160,
617 <https://doi.org/10.1016/j.atmosres.2015.11.018>, 2016.

618 Kerminen, V. M., Ojanen, C., Pakkanen, T., Hillamo, R., Aurela, M., and Meriläinen, J.:
619 Low-molecular-weight dicarboxylic acids in an urban and rural atmosphere, *J. Aerosol Sci.*, 31,
620 349-362, [https://doi.org/10.1016/S0021-8502\(99\)00063-4](https://doi.org/10.1016/S0021-8502(99)00063-4), 2000.

621 Kundu, S., Kawamura, K., Andreae, T. W., Hoffer, A., and Andreae, M. O.: Molecular distributions of
622 dicarboxylic acids, ketocarboxylic acids and α -dicarbonyls in biomass burning aerosols: implications
623 for photochemical production and degradation in smoke layers, *Atmos. Chem. Phys.*, 10, 2209–2225,
624 <https://doi.org/10.5194/acp-10-2209-2010>, 2010.

625 Kunwar, B., and Kawamura, K.: Seasonal distributions and sources of low molecular weight
626 dicarboxylic acids, α -oxocarboxylic acids, pyruvic acid, α -dicarbonyls and fatty acids in ambient
627 aerosols from subtropical Okinawa in the western Pacific Rim, *Environ. Chem.*, 11, 673-689,
628 <http://dx.doi.org/10.1071/EN14097>, 2014.

629 Kunwar, B., Kawamura, K., Fujiwara, S., Fu, P. Q., Miyazaki, Y., and Pokhrel, A.: Dicarboxylic acids,
630 oxocarboxylic acids and α -dicarbonyls in atmospheric aerosols from Mt. Fuji, Japan: Implication for
631 primary emission versus secondary formation, *Atmos. Res.*, 221, 58-71,
632 <https://doi.org/10.1016/j.atmosres.2019.01.021>, 2019.

633 Legrand, M., and De Angelis, M.: Light carboxylic acids in Greenland ice: A record of past forest fires
634 and vegetation emissions from the boreal zone, *J. Geophys. Res.-Atmos.*, 101, 4129-4145,
635 <https://doi.org/10.1029/95JD03296>, 1996.

636 Legrand, M., Preunkert, S., Oliveira, T., Pio, C. A., Hammer, S., Gelencsér, A., And, K. G., and Laj, P.:
637 Origin of C2–C5 dicarboxylic acids in the European atmosphere inferred from year-round aerosol study
638 conducted at a west-east transect, *J. Geophys. Res.-Atmos.*, 112, D23S07,
639 <https://doi.org/10.1029/2006JD008019>, 2007.

640 Li, J. J., Li, J., Wang, G. H., Zhang, T., Dai, W. T., Ho, K. F., Wang, Q., Shao, Y., Wu, C., and Li, L.:
641 Molecular characteristics of organic compositions in fresh and aged biomass burning aerosols, *Sci.*
642 *Total Environ.*, 741, 140247, <https://doi.org/10.1016/j.scitotenv.2020.140247>, 2020.

643 Li, J. J., Li, J., Wang, G. H., Ho, K. F., Dai, W. T., Zhang, T., Wang, Q., Wu, C., Li, L., Li, L., and
644 Zhang, Q.: Effects of atmospheric aging processes on in vitro induced oxidative stress and chemical
645 composition of biomass burning aerosols, *J. Hazard. Mater.*, 401, 123750,
646 <https://doi.org/10.1016/j.jhazmat.2020.123750>, 2021.

647 Lim, Y. B., Tan, Y., and Turpin, B. J.: Chemical insights, explicit chemistry, and yields of secondary
648 organic aerosol from OH radical oxidation of methylglyoxal and glyoxal in the aqueous phase, *Atmos.*
649 *Chem. Phys.*, 13, 8651-8667, <https://doi.org/10.5194/acp-13-8651-2013>, 2013.

650 Lim, C. Y., Hagan, D. H., Coggon, M. M., Koss, A. R., Sekimoto, K., de Gouw, J., Warneke, C., Cappa,
651 C. D., and Kroll J. H.: Secondary organic aerosol formation from the laboratory oxidation of biomass

652 burning emissions. *Atmos. Chem. Phys.*, 19, 12797–12809, <https://doi.org/10.5194/acp-19-12797-2019>,
653 2019.

654 Mao, J., Ren, X., Brune, W. H., Olson, J. R., Crawford, J. H., Fried, A., Huey, L. G., Cohen, R. C.,
655 Heikes, B., Singh, H. B., Blake, D. R., Sachse, G. W., Diskin, G. S., Hall, S. R., and Shetter, R. E.:
656 Airborne measurement of OH reactivity during INTEX-B, *Atmos. Chem. Phys.*, 9, 163–173,
657 <https://doi.org/10.5194/acp-9-163-2009>, 2009.

658 Meng, J. J., Wang, G. H., Li, J. J., Cheng, C. L., Ren, Y. Q., Huang, Y., Cheng, Y. T., Cao, J. J., and
659 Zhang, T.: Seasonal characteristics of oxalic acid and related SOA in the free troposphere of Mt. Hua,
660 central China: Implications for sources and formation mechanisms, *Sci. Total Environ.*, 493, 1088–1097,
661 <https://doi.org/10.1016/j.scitotenv.2014.04.086>, 2014.

662 Meng, J. J., Wang, G. H., Hou, Z. F., Liu, X. D., Wei, B. J., Wu, C., Cao, C., Wang, J. Y., Li, J. J., Cao,
663 J. J., Zhang, E., Dong, J., Ge, S. S., and Xie, Y. N.: Molecular distribution and stable carbon isotopic
664 compositions of dicarboxylic acids and related SOA from biogenic sources in the summertime
665 atmosphere of Mt. Tai in the North China Plain, *Atmos. Chem. Phys.*, 18, 15069–15086,
666 <https://doi.org/10.5194/acp-18-15069-2018>, 2018.

667 Meng, J. J., Liu, X. D., Hou, Z. F., Yi, Y. N., Yan, L., Li, Z., Cao, J. J., Li, J. J., and Wang, G. H.:
668 Molecular characteristics and stable carbon isotope compositions of dicarboxylic acids and related
669 compounds in the urban atmosphere of the North China Plain: Implications for aqueous phase
670 formation of SOA during the haze periods, *Sci. Total Environ.*, 705, 135256,
671 <https://doi.org/10.1016/j.scitotenv.2019.135256>, 2020.

672 Miyazaki, Y., Kimitaka, K., and Sawano, M.: Size distributions and chemical characterization of
673 water-soluble organic aerosols over the western North Pacific in summer, *J. Geophys. Res.-Atmos.*, 115,
674 D23210, <https://doi.org/10.1029/2010JD014439>, 2010.

675 Mkoma, S. L., and Kawamura, K.: Molecular composition of dicarboxylic acids, ketocarboxylic acids,
676 α -dicarbonyls and fatty acids in atmospheric aerosols from Tanzania, East Africa during wet and dry
677 seasons, *Atmos. Chem. Phys.*, 13, 2235–2251, <https://doi.org/10.5194/acp-13-2235-2013>, 2013.

678 Myriokefalitakis, S., Tsigaridis, K., Mihalopoulos, N., Sciare, J., Nenes, A., Kawamura, K., Segers, A.,
679 and Kanakidou, M.: In-cloud oxalate formation in the global troposphere: a 3-D modeling study, *Atmos.*
680 *Chem. Phys.*, 11, 5761–5782, <https://doi.org/10.5194/acp-11-5761-2011>, 2011.

681 Narukawa, M., Kawamura, K., Takeuchi, N., and Nakajima, T.: Distribution of dicarboxylic acids and
682 carbon isotopic compositions in aerosols from 1997 Indonesian forest fires, *Geophys. Res. Lett.*, 26,
683 3101–3104, <https://doi.org/10.1029/1999GL010810>, 1999.

684 Narukawa, M., Kawamura, K., Li, S. M., and Bottenheim, J. W.: Dicarboxylic acids in the arctic
685 aerosols and snowpacks collected during ALERT 2000, *Atmos. Environ.*, 36, 2491–2499,
686 [https://doi.org/10.1016/S1352-2310\(02\)00126-7](https://doi.org/10.1016/S1352-2310(02)00126-7), 2002.

687 Narukawa, M., Kawamura, K., Anlauf, K. G., and Barrie, L. A.: Fine and coarse modes of dicarboxylic
688 acids in the Arctic aerosols collected during the Polar Sunrise Experiment 1997, *J. Geophys. Res.-Atm.*,
689 108, 4575, <https://doi.org/10.1029/2003JD003646>, 2003.

690 Niu, X. Y., Li, J. J., Wang, Q. Y., Ho, S. S. H., Sun, J., Li, L., Cao, J. J., and Ho, K. F.: Characteristics
691 of fresh and aged volatile organic compounds from open burning of crop residues, *Sci. Total Environ.*,
692 726, 138545, <https://doi.org/10.1016/j.scitotenv.2020.138545>, 2020.

693 Pavuluri, C. M., Kawamura, K., and Swaminathan, T.: Water-soluble organic carbon, dicarboxylic acids,
694 ketoacids, and α -dicarbonyls in the tropical Indian aerosols, *J. Geophys. Res.-Atm.*, 115, D11302,
695 <https://doi.org/10.1029/2009JD012661>, 2010.

696 Pavuluri, C. M., and Kawamura, K.: Enrichment of ¹³C in diacids and related compounds during
697 photochemical processing of aqueous aerosols: New proxy for organic aerosols aging, *Sci. Rep.*, 6,
698 36467, <https://doi.org/10.1038/srep36467>, 2016.

699 Reid, J. S., Koppmann, R., Eck, T. F., Eleuterio, D. P., Holben, B. N., Reid, E. A., and J., Z.: A Review
700 of biomass burning emissions Part II: Intensive physical properties of biomass burning particles.,
701 *Atmos. Chem. Phys.*, 5 799–825, <https://doi.org/10.5194/acp-5-827-2005>, 2005.

702 Rogge, W. F., Hildemann, L. M., Mazurek, M. A., Cass, G. R., and Simoneit, B. R.: Sources of fine
703 organic aerosol. 1. Charbroilers and meat cooking operations, *Environ. Sci. Technol.*, 25, 1112-1125,
704 <https://doi.org/10.1021/es00018a015>, 1991.

705 Rogge, W. F., Hildemann, L. M., Mazurek, M. A., Cass, G. R., and Simoneit, B. R.: Sources of fine
706 organic aerosol. 2. Noncatalyst and catalyst-equipped automobiles and heavy-duty diesel trucks,
707 *Environ. Sci. Technol.*, 27, 636-651, <https://doi.org/10.1021/es00041a007>, 1993.

708 Rogge, W. F., Hildemann, L. M., and Mazurek, M. A.: Sources of fine organic aerosol .6.
709 Cigarette-smoke in the urban atmosphere, *Environ. Sci. Technol.*, 28, 1375–1388,
710 <https://doi.org/10.1021/Es00056a030>, 1994.

711 Sakugawa, H., and Kaplan, I. R.: Stable carbon isotope measurements of atmospheric organic acids in
712 Los Angeles, California, *Geophys. Res. Lett.*, 22, 1509-1512, <https://doi.org/10.1029/95GL01359>, 1995.

713 Samy, S., and Zielinska, B.: Secondary organic aerosol production from modern diesel engine
714 emissions, *Atmos. Chem. Phys.*, 10, 609-625, <https://doi.org/10.5194/acp-10-609-2010>, 2010.

715 Sato, K., Hatakeyama, S., and Imamura, T.: Secondary organic aerosol formation during the
716 photooxidation of toluene: NO_x dependence of chemical composition, *J. Phys. Chem. A*, 111,
717 9796-9808, <https://doi.org/10.1021/jp071419f>, 2007.

718 Schauer, J. J., Kleeman, M. J., Cass, G. R., and Simoneit, B. R. T.: Measurement of emissions from air
719 pollution sources.3. C₁–C₂₉ organic compounds from fireplace combustion of wood, *Environ. Sci.*
720 *Technol.*, 35, 1716–1728, <https://doi.org/10.1021/es001331e>, 2001.

721 Song, J. W., Zhao, Y., Zhang, Y. Y., Fu, P. Q., Zheng, L. S., Yuan, Q., Wang, S., Huang, X. F., Xu, W. H.,
722 Cao, Z. X., Gromov, S., and Lai, S.: Influence of biomass burning on atmospheric aerosols over the
723 western South China Sea: Insights from ions, carbonaceous fractions and stable carbon isotope ratios,
724 *Environ. Pollut.*, 242, 1800-1809, <https://doi.org/10.1016/j.envpol.2018.07.088>, 2018.

725 Sorathia, F., Rajput, P., and Gupta, T.: Dicarboxylic acids and levoglucosan in aerosols from
726 Indo-Gangetic Plain: Inferences from day night variability during wintertime, *Sci. Total Environ.*, 624,
727 451-460, <https://doi.org/10.1016/j.scitotenv.2017.12.124>, 2018.

728 Sorooshian, A., Ng, N. L., Chan, A. W. H., Feingold, G., Flagan, R. C., and Seinfeld, J. H.: Particulate
729 organic acids and overall water-soluble aerosol composition measurements from the 2006 Gulf of
730 Mexico Atmospheric Composition and Climate Study (GoMACCS), *J Geophys. Res.-Atmos.*, 112,
731 D13201, <https://doi.org/10.1029/2007JD008537>, 2007.

732 Tao, S., Ru, M. Y., Du, W., Zhu, X., Zhong, Q. R., Li, B. G., Shen, G. F., Pan, X. L., Meng, W. J., Chen,
733 Y. L., Shen, H. Z., Lin, N., Su, S., Zhuo, S. J., Huang, T. B., Xu, Y., Yun, X., Liu, J. F., Wang, X. L., Liu,
734 W. X., Cheng, H. F., and Zhu, D. Q.: Quantifying the rural residential energy transition in China from
735 1992 to 2012 through a representative national survey, *Nat. Energy*, 3, 567–573,
736 <https://doi.org/10.1038/s41560-018-0158-4>, 2018.

737 Tian, J., Watson, J. G., Han, Y. M., Ni, H. Y., Chen, L. W. A., Wang, X. L., Huang, R. J., Moosmüller,
738 H., Chow, J. C., and Cao, J. J.: A biomass combustion chamber: Design, evaluation, and a case study of
739 wheat straw combustion emission tests, *Aerosol Air Qual. Res.*, 15, 2104-2114,

740 <https://doi.org/10.4209/aaqr.2015.03.0167>, 2015.

741 Wang, G. H., Niu, S. L., Liu, C., and Wang, L. S.: Identification of dicarboxylic acids and aldehydes of
742 PM₁₀ and PM_{2.5} aerosols in Nanjing, China, *Atmos. Environ.*, 36, 1941–1950,
743 [https://doi.org/10.1016/S1352-2310\(02\)00180-2](https://doi.org/10.1016/S1352-2310(02)00180-2), 2002.

744 Wang, G. H., Kawamura, K., Watanabe, T., Lee, S. C., Ho, K. F., and Cao, J. J.: High loadings and
745 source strengths of organic aerosols in China, *Geophys. Res. Lett.*, 33, L22801,
746 <https://doi.org/10.1029/2006GL027624>, 2006.

747 Wang, G. H., Kawamura, K., Cheng, C. L., Li, J. J., Cao, J. J., Zhang, R., Zhang, T., Liu, S. X., and
748 Zhao, Z. Z.: Molecular distribution and stable carbon isotopic composition of dicarboxylic acids,
749 ketocarboxylic acids, and alpha-dicarbonyls in size-resolved atmospheric particles from Xi'an City,
750 China, *Environ. Sci. Technol.*, 46, 4783–4791, <https://doi.org/10.1021/es204322c>, 2012.

751 Wang, H. B., and Kawamura, K.: Stable carbon isotopic composition of low-molecular-weight
752 dicarboxylic acids and ketoacids in remote marine aerosols, *J. Geophys. Res.-Atom.*, 111, D07304,
753 <https://doi.org/10.1029/2005JD006466>, 2006.

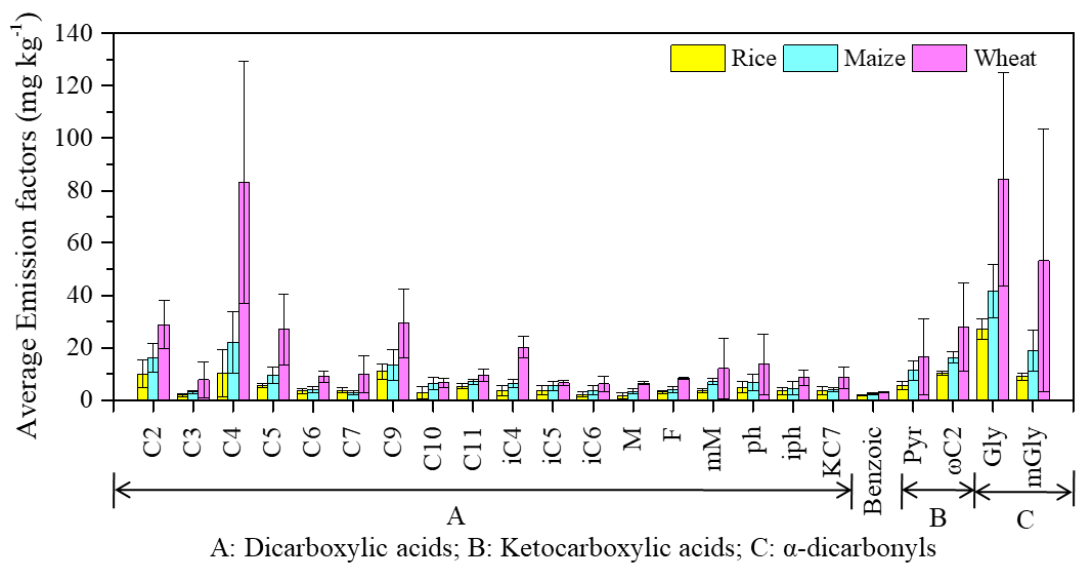
754 Warneck, P.: In-cloud chemistry opens pathway to the formation of oxalic acid in the marine
755 atmosphere, *Atmos. Environ.*, 37, 2423–2427, [https://doi.org/10.1016/S1352-2310\(03\)00136-5](https://doi.org/10.1016/S1352-2310(03)00136-5), 2003.

756 Watson, J. G., Cao, J. J., Chen, L. W. A., Wang, Q. Y., and Chow, J. C.: Gaseous, PM_{2.5} mass, and
757 speciated emission factors from laboratory chamber peat combustion, *Atmos. Chem. Phys.*, 19,
758 14173–14193, <https://doi.org/10.5194/acp-19-14173-2019>, 2019.

759 Yasmeen, F., Sauret, N., Gal, J. F., Maria, P. C., Massi, L., Maenhaut, W., and Claeys, M.:
760 Characterization of oligomers from methylglyoxal under dark conditions: a pathway to produce
761 secondary organic aerosol through cloud processing during nighttime, *Atmos. Chem. Phys.*, 10,
762 3803–3812, <https://doi.org/10.5194/acp-10-3803-2010>, 2010.

763 Zhang, Y. L., Kawamura, K., Cao, F., and Lee, M.: Stable carbon isotopic compositions of
764 low-molecular-weight dicarboxylic acids, oxocarboxylic acids, α -dicarbonyls, and fatty acids, *J.*
765 *Geophys. Res: Atmos.*, 3707–3717, <https://doi.org/10.1002/2015JD024081>, 2016.

766 Zhao, W. Y., Kawamura, K., Yue, S. Y., Wei, L. F., Ren, H., Yan, Y., Kang, M. J., Li, L. J., Ren, L. J.,
767 Lai, S. C., Li, J., Sun, Y. L., Wang, Z. F., and Fu, P. Q.: Molecular distribution and compound-specific
768 stable carbon isotopic composition of dicarboxylic acids, oxocarboxylic acids and α -dicarbonyls in
769 PM_{2.5} from Beijing, China, *Atmos. Chem. Phys.*, 18, 2749–2767,
770 <https://doi.org/10.5194/acp-18-2749-2018>, 2018.

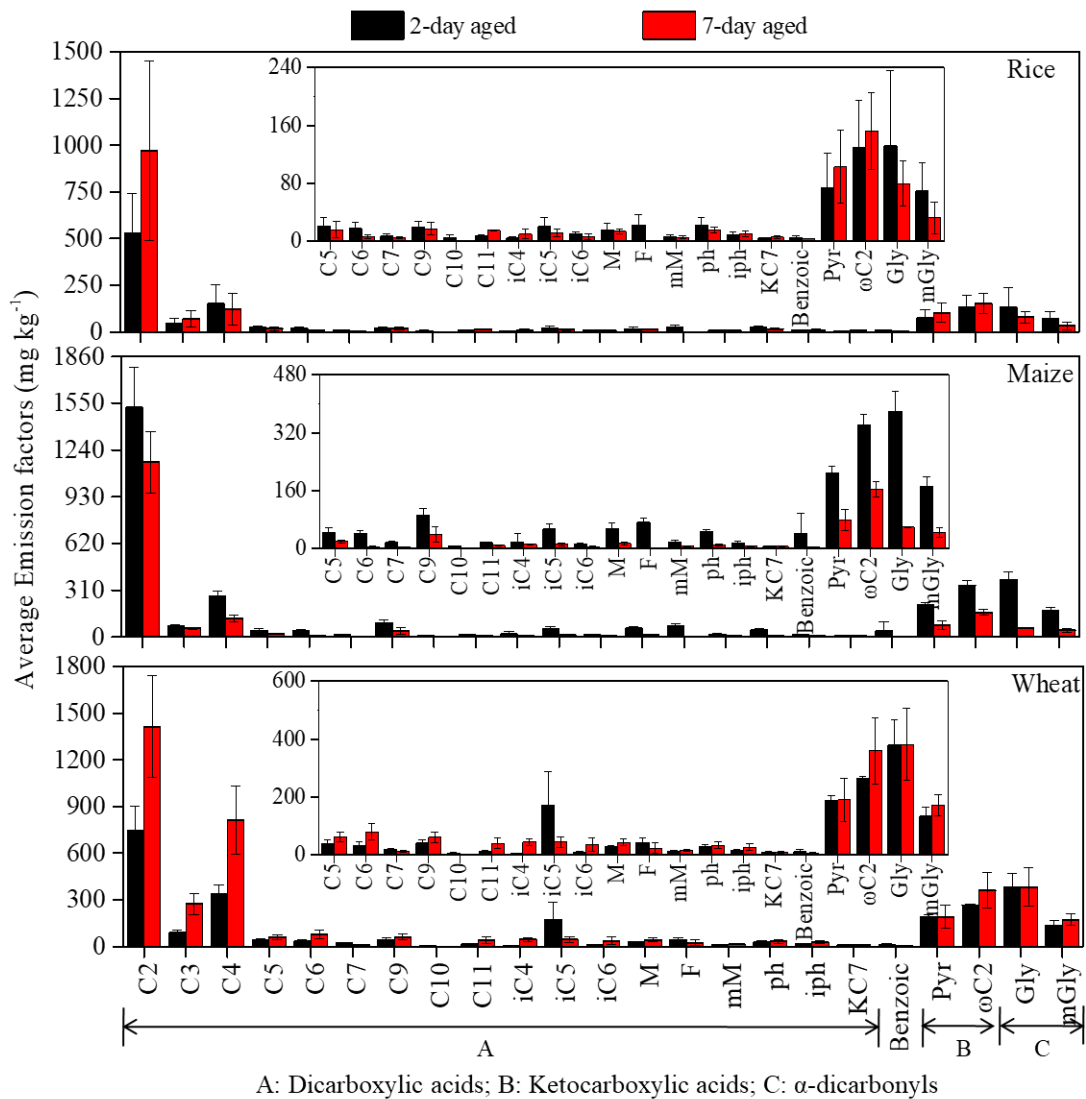


771

772

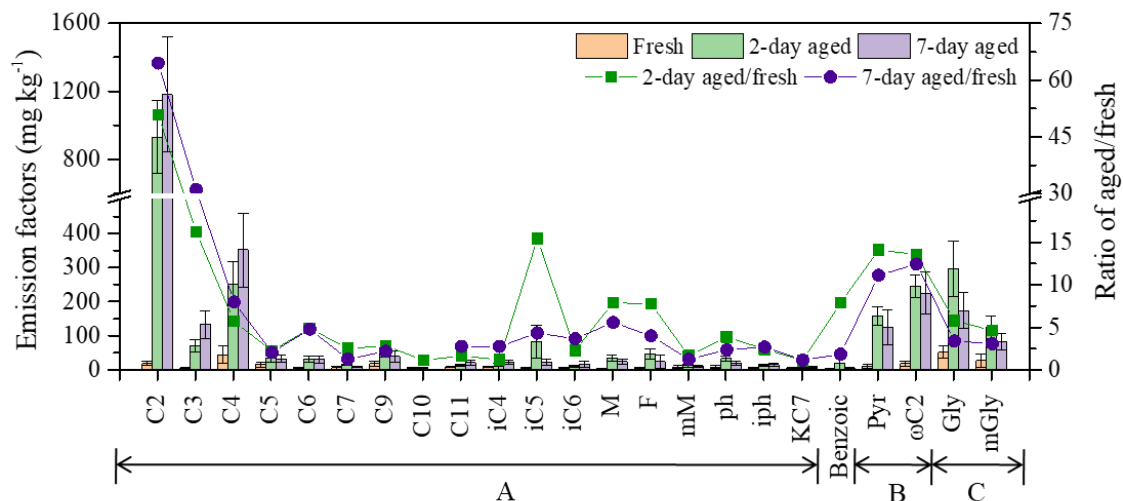
773

Figure 1 Average emission factors of dicarboxylic acids and related compounds in fresh PM_{2.5} aerosols from biomass burning.



774
775
776
777
778

Figure 2 Comparison between 2- and 7-day aged average PM_{2.5} emission factors of A: dicarboxylic acids, B: ketocarboxylic acids, and C: α-carbonyls for laboratory combustion of rice, maize, and wheat straw.



A: Dicarboxylic acids; B: Ketocarboxylic acids; C: α -dicarbonyls

779

780

Figure 3 Average emission factors of dicarboxylic acids and related compounds from

781

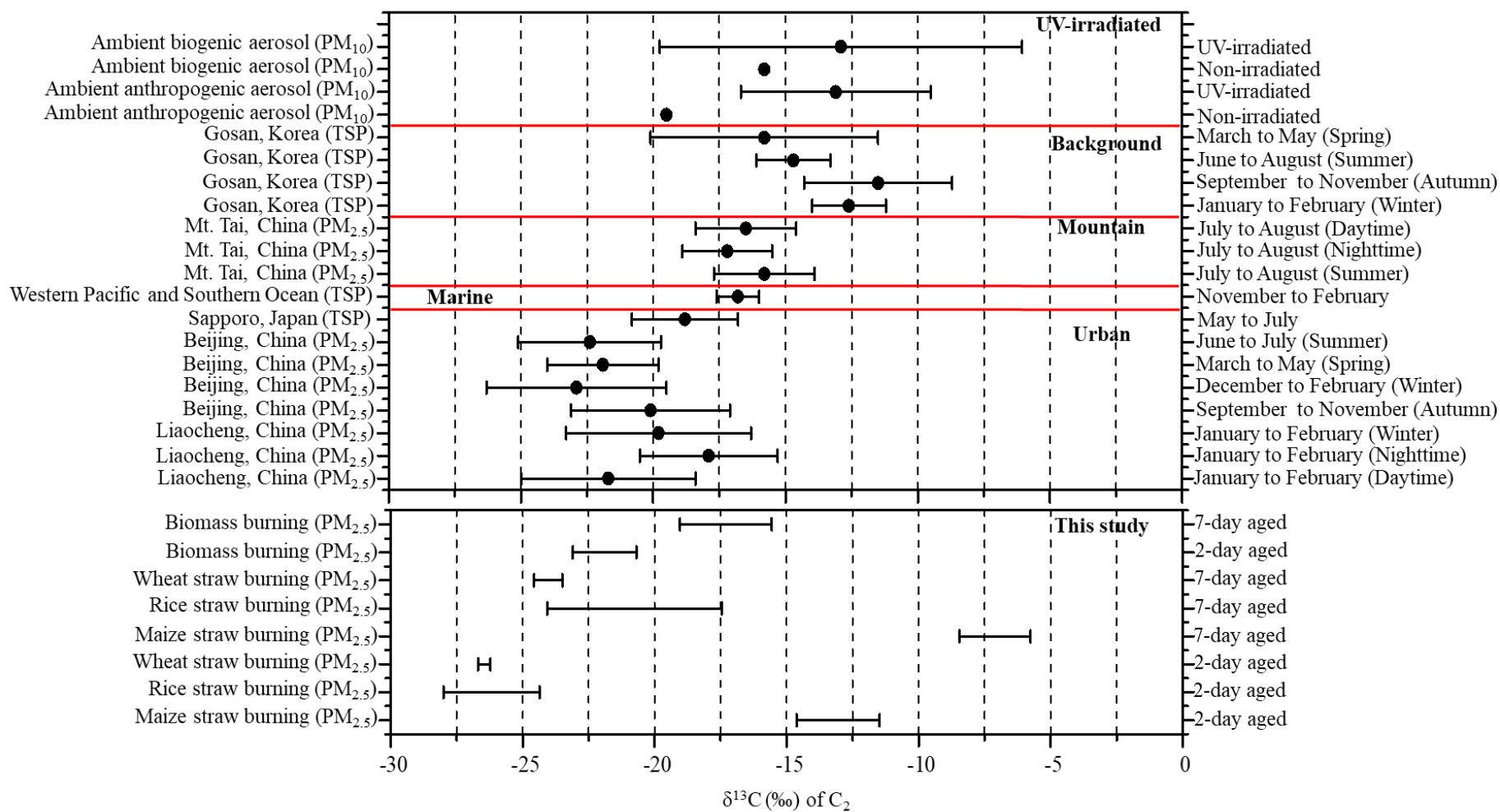
biomass burning experiment for the fresh, 2- and 7-day aged PM_{2.5} aerosols. The

782

squares and dots denote the ratios of aged to fresh (A/F) sample for the dicarboxylic

783

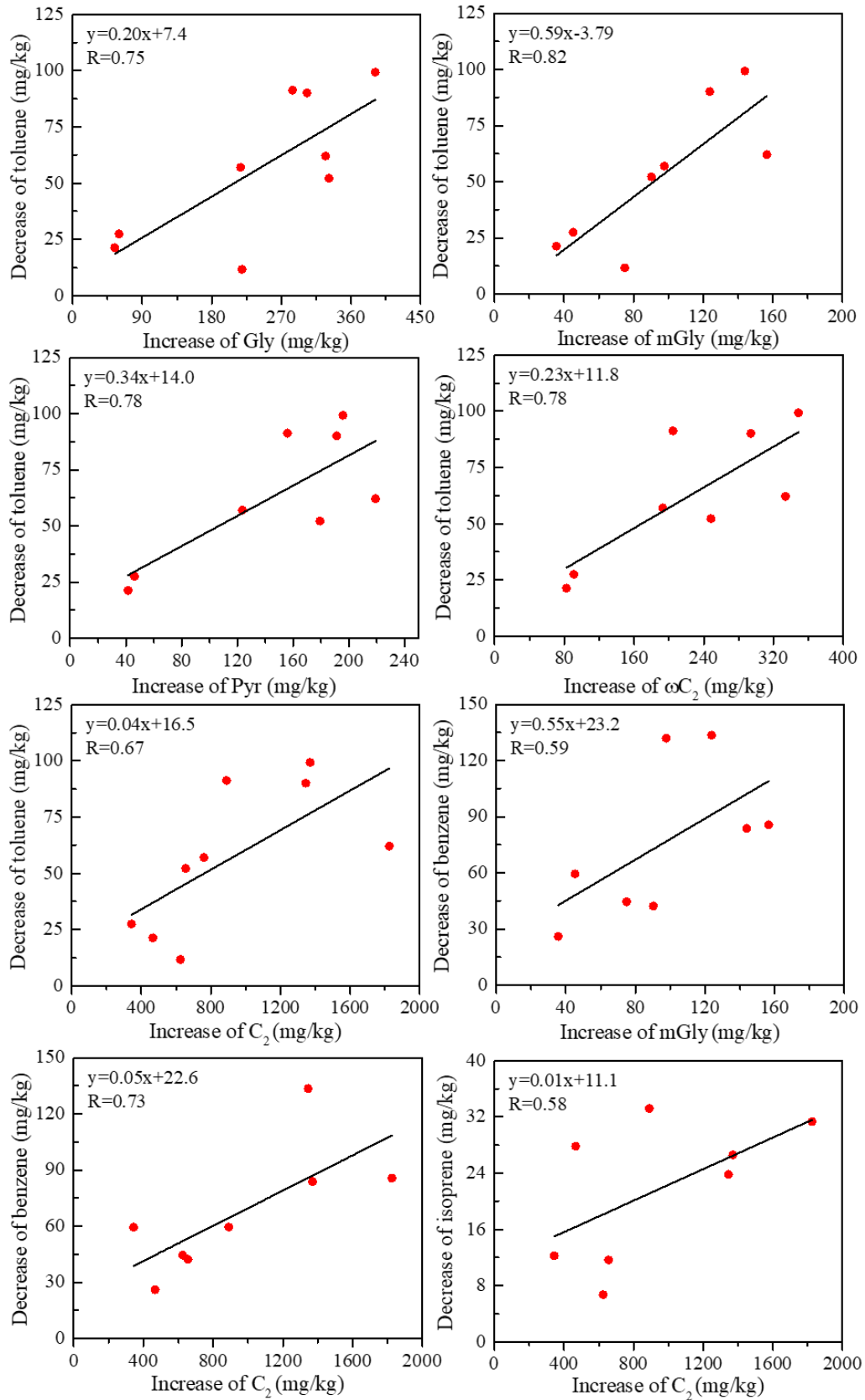
acids and related compounds after 2- and 7-day aging.



784

785

Figure 4 Stable carbon isotope ratios ($\delta^{13}\text{C}$, ‰) of C_2 in aerosols from selected environments.



786

787 Figure 5 Regressions between the decreases of specific VOCs (toluene, benzene and

788 isoprene) and increases of C₂ and its intermediates methylglyoxal (mGly), Glyoxal,

789 (Gly), Pyruvic acid (Pyr) and Glyoxylic (ωC_2).

790 Table 1 Emission factors (EFs, mg kg⁻¹) of fresh and aged dicarboxylic acids and related compounds from rice, maize and wheat straw burning.

Compounds	Rice-2 day aged		Rice-7 day aged		Maize-2 day aged		Maize-7 day aged		Wheat-2 day aged		Wheat-7 day aged	
	Fresh	2-d aged	Fresh	7-d aged	Fresh	2-d aged	Fresh	7-d aged	Fresh	2-d aged	Fresh	7-d aged
I. Dicarboxylic acids												
Oxalic, C ₂	5.1±0.9	527±214	15±10	971±482	8.1±2.2	1522±268	24±8.8	1158±202	18±15	742±160	39±3.4	1412±328
Malonic, C ₃	2.4	46±26	1.4±0.7	70±42	3.6	74±8.4	2.7±0.6	56±9.0	12±13	89±18	3.6±0.8	273±70
Succinic, C ₄	<DL ^a	152±100	10±9.0	120±85	9.3±12	268 ±35	35±12	124±23	44±72	335±62	122±21	813 ±217
Glutaric, C ₅	<DL	21±12	5.4±0.8	16±11	8.9	44±13	10±3.1	20±2.8	28±23	41±12	27±3.7	61±16
Adipic, C ₆	<DL	18± 8.6	3.5±0.9	6.4±2.2	<DL	42±6.4	4.1±1.1	5.8±0.7	12	33 ±11	5.5±2.2	79±28
Pimelic, C ₇	5.0	7.4± 2.7	2.4±0.9	4.9±1.7	<DL	18±2.1	2.8±0.9	5.5±0.3	16±12	21±3.1	4.0±1.6	13±2.8
Azelaic, C ₉	11±1.8	19±8.8	11±3.9	18±8.4	10±3.2	91±21	17±8.4	39±22	23±20	41 ±12	35±6.5	61±19
Sebacic, C ₁₀	2.8±2.3	5.0±4.6	<DL	<DL	6.2±2.3	7.0±0.5	<DL	<DL	6.6±1.7	5.7±3.1	<DL	<DL
Undecanedioic, C ₁₁	<DL	7.6±1.5	5.4±1.1	15±1.2	6.7±1.2	18±1.5	7.5±0.8	8.9±2.1	11.2	14±2.8	7.9±2.4	40±19
Methylmalonic, iC ₄	3.6	4.8±1.8	3.7±1.9	10±6.8	3.8±0.2	19±22	9.1±2.9	11±2.1	<DL	5.7 ±1.4	20±4.2	46±12
Mehtylsuccinic, iC ₅	<DL	20±13	3.8±1.7	12±5.5	<DL	54±16	5.6±1.8	12±3.5	<DL	172±114	6.6 ±1.0	45±19
Methylglutaric, iC ₆	<DL	9.8± 2.7	2.1 ±1.0	6.1±3.6	3.4	12±3.4	4.0±1.9	5.7±1.4	7.4±4.9	8.3±2.9	5.1±1.0	37±23
Maleic, M	<DL	16±8.9	1.6±1.2	14±3.5	2.8±1.1	56±14	4.0±1.0	14±3.6	9.6	29±3.8	3.4±0.6	43±11
Fumaric, F	<DL	22±15	3.1±0.6	<DL	<DL	73±13	4.0±1.1	<DL	13	43±15	3.6±0.3	24±19
Methylmaleic, mM	4.5±0.7	6.7± 2.1	2.5±0.8	5.6±2.4	7.3±0.5	18±5.3	6.6±1.9	6.5±1.2	19± 22	12±3.4	5.5±0.8	16±4.7
Phthalic, Ph	4.0±0.5	23±10	5.8 ±3.5	16±4.3	3.8±1.0	47±6.5	10±5.4	11±2.6	10± 12	29±6.9	17±12	33±12
Isophthalic, iPh	4.1	8.7±3.8	2.9±1.3	11±3.6	3.9	17±3.9	5.2±2.7	7.3±1.3	9.7±2.7	16±2.6	7.6 ±3.1	27±11

Ketopimelic, kC ₇	<DL	4.4±0.6	3.6±1.6	6.0±1.8	<DL	6.5±1.9	3.9±0.7	6.3±0.6	13±7.6	9.3 ±2.5	4.5 ±0.4	8.9±3.1
Subtotal	43±6.2	919±437	83±41	1300±66 5	78±23	2386±440	155±55	1491±279	252±206	1645±437	318±64	3032±814
II. Ketocarboxylic acids												
Pyruvic acid, Pyr	4.6	74±48	6.5±3.1	103±50	8.1±3.5	210±17	15±4.3	79±29	21±25	189±15	13±4.0	190±75
Glyoxylic, ωC ₂	11±0.3	129±65	9.6±1.3	152±53	16±2.0	341±30	17±2.5	164±21	33±27	265±4.9	23±6.3	359±114
Subtotal	16±0.4	203±113	16±4.4	255±103	24±5.5	551±48	32±6.8	243±50	53±52	454±20	35±10	550±189
III. α-Dicarbonyls												
Glyoxal, Gly	32±1.1	132±104	22±6.7	79±31	39±8.6	380±54	44±12	60±1.7	102±71	380±87	67±11	382±125
Methylglyoxal, mGly	15±0.5	70±39	2.8±2.2	33±22	30±13	172±28	7.6 ±2.6	46±13	91±96	135±31	16±4.0	172±37
Subtotal	47±1.6	202±143	25±8.9	112±53	69±22	551±82	52±14	106±15	192±167	515±118	83±15	554±161
Benzoic acid, Ha	<DL	5.4±2.1	1.9±0.2	3.8±0.3	<DL	42±57	2.5±0.4	4.0±1.1	<DL	12±7.8	3.1±0.3	6.0 ±2.0
Total detected organics	105±8.2	1329±695	127±54	1671±821	171±50	3530±626	241±76	1844±344	498±425	2626±583	439±90	4141±1166

^a<DL denotes emissions below method detection limit (MDL).

791 Table 2 Comparison of mass ratios of C_3/C_4 , C_2/C_4 , $C_2/\text{total diacids}$, $\omega C_2/C_2$ and Gly/mGly in fresh and aged aerosols collected from biomass
 792 burning with the different locations around the World

	Sampling site	Particle size	C_3^1/C_4	C_2/C_4	$C_2/\text{total diacids}$	$\omega C_2/C_2$	Gly/mGly	References
Mountain	Mt. Hua	PM ₁₀	2.0	10.7	0.6	0.06	0.6	Meng et al. (2014)
	Mt. Tai	TSP	0.8	5.3	0.6	0.1	0.5	Kawamura et al. (2013)
	Mt. Fuji	TSP	0.6	1.9	0.5	0.05	1.2	Kunwar et al. (2019)
	Tokyo, Japan	TSP	1.0	4.2	0.5	0.2	0.7	Kawamura et al. (2005)
Urban	Liaocheng, China	PM _{2.5}	0.4	3.6	0.6	0.1	1.0	Meng et al. (2020)
	Fairbanks	PM _{2.5}	1.2	4.2	0.5	0.1	1.4	Deshmukh et al. (2018)
	DoiAngKhang, Thailand	PM _{2.5}	0.5	25.2	0.6	0.1	2.0	Boreddy et al. (2021)
	Beijing, China	PM _{2.5}	0.8	6.8	0.5	0.1	0.6	Zhao et al. (2018)
	Xi'an, China	PM ₁₀	0.8	10.4	0.6	0.1	0.7	Cheng et al. (2013)
Marine area	North Pacific	TSP	1.4	5.3	0.5	0.01	2.0	Kawamura et al. (1993)
	Eastern North Pacific	TSP	1.1	4.3	0.5	0.004	0.2	Hoque et al. (2020)
	Western North to equatorial Pacific	TSP	3.9	14.3	0.6	/	/	Kawamura et al. (1999)
Island	Okinawa	TSP	1.9	15.5	0.8	0.06	0.5	Kunwar et al. (2014)
	Motor Exhausts		0.35					Kawamura et al. (1987)
Laboratory simulation	Siberian (biomass burning, chamber)	PM _{2.5}	<0.03	<1	/	/	/	Kalogridis et al. (2018)
	Fresh (biomass burning, chamber)	PM _{2.5}	0.2	0.7	0.1	1.3	3.8	
	2-day aged (biomass burning, chamber)	PM _{2.5}	0.3	3.8	0.6	0.3	2.3	This study
	7-day aged (biomass burning, chamber)	PM _{2.5}	0.5	6.4	0.6	0.2	2.0	

793 ¹ See compound list in Table 1

794 Table 3 Stable carbon isotope ratios ($\delta^{13}\text{C}$, ‰) of C_2 in atmospheric aerosols from selected
 795 locations

Sampling site	Particle size	Min ¹	Max	Ave.	Std.	Sampling interval	References
Urban							
Liaocheng, China	PM _{2.5}	-31.8	-16.6	-21.7	3.3	Jan. to Feb. (Daytime)	Meng et al. (2020)
	PM _{2.5}	-26.5	-14.1	-17.9	2.6	Jan. to Feb.	
	PM _{2.5}	-31.8	-14.1	-19.8	3.5	Jan. to Feb. (Winter)	
Beijing, China	PM _{2.5}	-23.7	-15.0	-20.1	3.0	Sep. to Nov.	Zhao et al. (2018)
	PM _{2.5}	-27.2	-14.8	-22.9	3.4	Dec. to Feb. (Winter)	
	PM _{2.5}	-25.0	-16.6	-21.9	2.1	Mar. to May (Spring)	
Sapporo, Japan	PM _{2.5}	-27.0	-19.1	-22.4	2.7	Jun. to Jul. (Summer)	Aggarwal et al. (2008)
	TSP	-22.4	-14.0	-18.8	2.0	May to Jul.	
Marine							
Western Pacific and Southern Ocean	TSP	-27.1	-6.7	-16.8	0.8	Nov. to Feb.	Wang and Kawamura (2006)
Mountain							
Mt. Tai, China	PM _{2.5}	-19.4	-13.0	-15.8	1.9	Jul. to Aug. (Daytime)	Meng et al. (2018)
	PM _{2.5}	-20.1	-12.1	-17.2	1.7	Jul. to Aug.	
	PM _{2.5}	-20.1	-12.1	-16.5	1.9	Jul. to Aug. (Summer)	
Background							
Gosan, Korea	TSP	-15.0	-10.6	-12.6	1.4	Mar. to May (Spring)	Zhang et al. (2016)
	TSP	-14.1	-7.5	-11.5	2.8	Jun. to Aug.	
	TSP	-16.7	-13.2	-14.7	1.4	Sep. to Nov.	
	TSP	-20.5	-10.1	-15.8	4.3	Jan. to Feb. (Winter)	
UV-irradiated							
Ambient anthropogenic	PM ₁₀			-19.5		Non-irradiated	Pavuluri and Kawamura (2016)
Ambient biogenic aerosol	PM ₁₀			-13.1	3.6	UV-irradiated	
	PM ₁₀			-15.8		Non-irradiated	
	PM ₁₀			-12.9	6.9	UV-irradiated	
This study							
Maize straw	PM _{2.5}	-14.9	-12.1	-13.1	1.6	2-day aged	This study
Rice straw	PM _{2.5}	-28.2	-24.6	-26.2	1.8	2-day aged	
Wheat straw	PM _{2.5}	-26.7	-26.3	-26.5	0.2	2-day aged	
Maize straw	PM _{2.5}	-9.1	-6.0	-7.1	1.4	7-day aged	
Rice straw	PM _{2.5}	-23.7	-17.2	-20.8	3.3	7-day aged	
Wheat straw	PM _{2.5}	-24.6	-23.5	-24.0	0.5	7-day aged	
Biomass burning	PM _{2.5}	-23.3	-21.0	-21.9	1.2	2-day aged	
	PM _{2.5}	-19.1	-15.5	-17.3	1.7	7-day aged	

796 ¹Min, Max, Ave, and Std stand for minimum, maximum, arithmetic mean, and standard deviation.